Resonance and bifurcation in a discrete-time predator-prey system with Holling functional response

R. Khoshsiar Ghaziani[1] , W. Govaerts[2], C. Sonck[2,⋆]

[1] Department of Applied Mathematics, Shahrekord University, P.O. Box 115, Shahrekord, Iran, Khoshsiar@sci.sku.ac.ir
[2] Department of Applied Mathematics and Computer Science, Ghent University, Krijgslaan 281-S9, B-9000 Gent, Belgium, Willy.Govaerts@UGent.be, Charlotte.Sonck@UGent.be.

Keywords: iterated map, normal form, hyperbolic response, stable cycle.

Abstract. We perform a bifurcation analysis of a discrete predator-prey model with Holling functional response. We summarize stability conditions for the three kinds of fixed points of the map, further called F_1, F_2 and F_3 and collect complete information on this in a single scheme. In the case of F_2 we also compute the critical normal form coefficient of the flip bifurcation analytically. We further obtain new information about bifurcations of the cycles with periods $2, 3, 4, 5, 8$ and 16 of the system by numerical computation of the corresponding curves of fixed points and codim-1 bifurcations, using the software package MatContM. Numerical computation of the critical normal form coefficients of the codim-2 bifurcations enables us to determine numerically the bifurcation scenario around these points as well as possible branch switching to curves of codim-1 points. Using parameter-dependent normal forms, we compute codim-1 bifurcation curves that emanate at codim-2 bifurcation points in order to compute the stability boundaries of cycles with periods 4, 5, 8 and 16.

1 Introduction

Interactions of different species may take many forms such as competition, predation, parasitism and mutualism. One of the most important interactions is the predator-prey relationship. The dynamic relationship between predator and prey is one of the dominant subjects in mathematical ecology due to its universal existence and importance. For more details on different types of predator-prey systems we refer to [5] and the references cited therein. How predators respond to changes in prey availability (functional response) is an issue of particular importance. A functional response specifies the rate at which prey are consumed, per predator, as a function of the prey density. The type of functional response specified can greatly affect model predictions, see [20, 6].

⋆ Corresponding author.

Three general forms of functional response are commonly used in ecological models namely linear, hyperbolic, and sigmoidal. The linear functional (Lotka-Volterra) response specifies a directly proportional relationship between the consumption rate of an individual predator and the density of its prey. Holling [11] extended this to include a cap or limitation (Holling's type I), where there is an abrupt upper threshold representing predator satiation. The hyperbolic (respectively, sigmoid) functional response, most commonly known as Holling's type II (respectively type III) function, incorporate search rate and predator handling time to produce a smooth asymptotic curve.

Discrete-time predator-prey models go back at least to [21] where the classical discrete-time Lotka-Volterra model is introduced. They are further studied by many authors, see [4, 13, 14, 16, 22, 23, 25, 27–29]. For example, Sacker and von Bremen [27] propose a biological model for the genetic reproductive process and compute some invariant curves explicitly. Four typical discrete-time ecosystem models under the effects of periodic forcing have been studied in [28]. In a simple discrete-time predator-prey model with Holling's type I functional response, chaotic dynamics can occur [3].

In this paper we consider the general case of a discrete-time predator-prey system with Holling type II response. Our model is equivalent to model (30) in [25] and therefore to a special case of a model in [10] which itself is a discretization of a system studied in [26].

In [1] and [15] the same model is studied and we follow their notation. The main differences with these papers are that (a) we focus on results that have an immediate ecological meaning, (b) that we consider not only the map but also its iterates so that periodic orbits come into the picture much more prominently, and (c) that we rely heavily on advanced numerical methods, namely numerical continuation to obtain results that cannot be obtained analytically.

Point (a) means, for example, that we are interested mainly in stability and instability of fixed points of the map and its iterates. Contrary to what is done in [1, 15], the linear nature of the fixed points is of little interest to us. This leads to a simple classification of the stability and instability regions of all fixed points of the map that can be summarized in a global picture (Figure 2).

For (b) we remark that the only numerical illustrations in [1, 15] are orbit simulations. This does not allow to compute stability boundaries numerically.

In Section 2 we introduce the model and discuss the stability and bifurcations of its fixed points. We derive analytically the stability regions of all types of fixed points and their bifurcation behaviours. Moreover, we compute analytically the critical normal form coefficients in the case of the period doubling bifurcation to prove supercriticality. These results correct those in [1] and are consistent with those of [15]. In the degenerate case where the functional response reduces to a mass-action law, they were already obtained in [25, 23].

In Section 3 we numerically compute curves of codim-1 bifurcations and the critical normal form coefficients of codim-2 bifurcation points, using the MATLAB toolbox MATCONTM [8, 9]. These tools enable us to compute stability boundaries of different cycles. In particular, we determine the bifurcation scenario of

the map near an $R4$ resonance point, which involves stable and unstable 4-cycles as well as 8-cycles and 16-cycles. As an example of the power of the numerical methods we compute a region where a stable 8-cycle coexists with a stable 4-cycle. As another application we compute a branch of neutral saddle 3-cycles. We furthermore compute an Arnol'd tongue of period 5 and so find a parameter region where stable period-5 cycles exist.

In Section 4 we summarize our results and draw some conclusions.

2 Holling type II predator-prey system, existence and stability of its fixed points

The Lotka-Volterra predator-prey system (see e.g. [7, 17, 29, 30]) is a fundamental population model. More realistic predator-prey systems were introduced by Holling [11] using the three kinds of functional responses for different species to model the phenomena of predation. We first mention the continuous-time predator-prey model studied in [12] and later studied in a discretized version in [1]:

$$\begin{aligned} \dot{x}(t) &= \alpha_0 x(1-x) - \alpha \frac{mxy}{1+\epsilon x}, \\ \dot{y}(t) &= \left(\frac{mx}{1+\epsilon x} - \beta \right) y, \end{aligned} \tag{1}$$

where $\alpha_0, m, \alpha, \beta$ and $\epsilon > 0$ are parameters and $x(t)$, $y(t)$ represent the densities of the prey and the predator, respectively. α_0 is the intrinsic growth rate of the prey, m is a mass-action law constant, ϵ is a limitation parameter of the growth of the predator population for increasing prey density, $ax(1-x)$ is a logistic function and $\frac{mxy}{1+\epsilon x}$ is the Holling type II functional response, β and α denote the death rate of the predator and conversion, respectively.

In the case of a predator-prey system with non-overlapping generations this can be replaced by a discrete system

$$F : \begin{pmatrix} x \\ y \end{pmatrix} \mapsto \begin{pmatrix} ax(1-x) - \frac{bxy}{1+\epsilon x} \\ \frac{dxy}{1+\epsilon x} \end{pmatrix}, \tag{2}$$

where a, b, d are nonnegative parameters and $\epsilon > 0$. This model was studied in [1, 15]. We note that the parameter b can be absorbed by rescaling y. Thefore this is, from a bifurcation point of view, a three-parameter problem and we will indeed see that b does not appear in any bifurcation equations.

The bifurcation analysis of (2) naturally starts with fixed points. The fixed points of (2) are the solutions (x^*, y^*) to

$$ax^*(1-x^*) - \frac{bx^*y^*}{1+\epsilon x^*} = x^*, \quad \frac{dx^*y^*}{1+\epsilon x^*} = y^*.$$

The origin $F_1 = (0, 0)$ is always a fixed point of (2). Two further fixed points of the system are given by $F_2 = (\frac{a-1}{a}, 0)$ which is biologically possible for $a \geq 1$

and

$$F_3 = \left(\frac{1}{d-\epsilon}, \frac{d}{d-\epsilon} \left(\frac{a}{b} \left(1 - \frac{1}{d-\epsilon} \right) - \frac{1}{b} \right) \right). \tag{3}$$

We note that F_3 is biologically possible if its coordinates are nonnegative, i.e.,

$$\begin{array}{c} a > 1, \\ d \geq \epsilon + \frac{a}{a-1}. \end{array} \tag{4}$$

We start the local bifurcation analysis of the map (2) by linearization of F around each of its fixed points. The Jacobian matrix $J(x, y)$ is given by:

$$J(x,y) = \begin{pmatrix} a(1-2x) - \frac{by}{(1+\epsilon x)^2} & -\frac{bx}{1+\epsilon x} \\ \frac{dy}{(1+\epsilon x)^2} & \frac{dx}{1+\epsilon x} \end{pmatrix}. \tag{5}$$

The characteristic equation of $J(x, y)$ is given by

$$\lambda^2 - tr(J)\lambda + det(J) = 0, \tag{6}$$

where $tr(J) = a(1-2x) - \frac{by}{(1+\epsilon x)^2} + \frac{dx}{1+\epsilon x}$ and $det(J) = \frac{adx(1-2x)}{1+\epsilon x}$.

2.1 Stability of F_1

Proposition 1. *The fixed point F_1 is asymptotically stable for $0 \leq a < 1$. It loses stability via branching for $a = 1$ and there bifurcates to F_2.*

Proof. Eigenvalues of the Jacobian at F_1 are a and 0. So F_1 is stable if $a < 1$ and loses stability at $a = 1$. It remains to show that F_1 bifurcates to F_2 at $a = 1$. To do this we consider the matrix $(F_x - I|F_a)$, evaluated at F_1:

$$\begin{pmatrix} a-1 & 0 & 0 \\ 0 & -1 & 0 \end{pmatrix}. \tag{7}$$

When $a = 1$, this matrix is clearly rank deficient. We choose vectors ϕ_1 and ϕ_2 which form a basis for the null space of $J(F_1)$ and a vector ψ that spans the null space of $J(F_1)^T$. A possible choice is:

$$\phi_1 = (\frac{1}{\sqrt{2}}, 0, \frac{1}{\sqrt{2}})^T, \quad \phi_2 = (1,0,0)^T, \quad \psi = (1,0)^T.$$

Now we consider the *algebraic branching equation* (ABE), see [8],

$$c_{11}\alpha^2 + 2c_{12}\alpha\beta + c_{22}\beta^2 = 0, \tag{8}$$

where $c_{jk} =< \psi, F^0_{YY}\phi_j\phi_k >$ for $j, k = 1, 2$. Here the $2 \times 3 \times 3$ tensor F^0_{YY} of second derivatives of F with respect to the three variables x, y, a taken at $(0, 0)$ is given by:

$$F^0_{YY}(:,:,1) = \begin{pmatrix} -2a & -b & 1 \\ 0 & d & 0 \end{pmatrix}, \tag{9}$$

$$F^0_{YY}(:,:,2) = \begin{pmatrix} -b & 0 & 0 \\ d & 0 & 0 \end{pmatrix}, \tag{10}$$

$$F^0_{YY}(:,:,3) = \begin{pmatrix} 1 & 0 & 0 \\ 0 & 0 & 0 \end{pmatrix}. \tag{11}$$

We obtain $c_{11} = \frac{-2a+2}{2}$, $c_{12} = \frac{-2a+1}{\sqrt{2}}$, $c_{22} = -2a$. For $a = 1$, we obtain $c_{11} = 0$. So the discriminant of (8) is $\Delta = c_{12}^2 - c_{11}c_{22} = c_{12}^2 = \frac{1}{2} > 0$.

If $Y(s)$ is any branch of fixed points of (2) with $Y(s_0) = (0, 0, 1)$, then its derivative $Y_s(s_0)$ can be written as $Y_s(s_0) = \alpha\phi_1 + \beta\phi_2$ where α and β are scaled roots of (8). We find

$$Y_{1s} = (\frac{1}{\sqrt{2}}, 0, \frac{1}{\sqrt{2}})^T, \quad Y_{2s} = (0, 0, 1)^T.$$

The branch $X(s) = (0, 0, s)$ of F_1-equilibria has unit tangent vector $X_s = (0, 0, 1)^T$, i.e. Y_{2s}. Differentiation of the branch of F_2-equilibria w.r.t the parameter a leads to the vector $(\frac{1}{a^2}, 0, 1)^T$. When $a = 1$, the scaled tangent vector to this branch of is $(\frac{1}{\sqrt{2}}, 0, \frac{1}{\sqrt{2}})^T$, i.e. Y_{1s}. □

2.2 Stability of F_2

The Jacobian matrix of (2) at F_2 is given by

$$J(F_2) = \begin{pmatrix} 2 - a & \frac{b(1-a)}{a+\epsilon(a-1)} \\ 0 & \frac{d(a-1)}{a+\epsilon(a-1)} \end{pmatrix}. \tag{12}$$

Proposition 2. *The fixed point F_2 is asymptotically stable iff $a \in]1, 3[$ and $d < \epsilon + \frac{a}{a-1}$. Moreover, it loses stability:*

(i) via branching for $a = 1$ and there bifurcates to F_1.
(ii) via branching for $d = \epsilon + \frac{a}{a-1}$ and there bifurcates to F_3 if $1 < a < 3$.
(iii) via a supercritical flip for $a = 3$ if $d < \epsilon + \frac{3}{2}$.

Proof. The eigenvalues of $J(F_2)$ are $\lambda_1 = 2 - a$ and $\lambda_2 = \frac{d(a-1)}{a+\epsilon(a-1)}$. The fixed point F_2 is asymptotically stable iff $|\lambda_1| < 1$ and $|\lambda_2| < 1$, i.e. iff $a \in]1, 3[$ and $d < \epsilon + \frac{a}{a-1}$.

Boundary points of the stability region must satisfy one of three conditions: $a = 1$, $d = \epsilon + \frac{a}{a-1}$, or $a = 3$.

In the first case the conditions $d < \epsilon + \frac{a}{a-1}$ and $a < 3$ are satisfied for nearby values $a > 1$, hence this is a real stability boundary. In Proposition 1 we proved that this is a branch point and the new branch consists of F_1 points.

In the second case this is a stability boundary only if $1 < a < 3$. The Jacobian (12) then has an eigenvalue $+1$ and it is checked easily that these boundary points are also F_3 points.

In the third case, this is a stability boundary only if $d < \epsilon + \frac{3}{2}$. In this case $\lambda_1 = -1$ which means that F_2 loses stability via a period doubling point.

For supercriticality of the period doubling point it is sufficient to show that the corresponding critical normal form coefficient b,

$$b = \frac{1}{6}\left\langle p, C(q,q,q) + 3B(q,(I-A)^{-1}B(q,q))\right\rangle, \tag{13}$$

derived by center manifold reduction is positive, see [19], Ch. 8 and [8]. Here $A = J(F_2)$, and $B(.,.)$, $C(.,.,.)$ are the second and third order multilinear forms respectively, and p and q are the left and right eigenvectors of A for the eigenvalue -1, respectively. These vectors are normalized by $\langle p, q\rangle = 1$, $\langle q, q\rangle = 1$, where $\langle ..\rangle$ is the standard scalar product in $\mathbb{R}^2$. We obtain:

$$q = \begin{pmatrix} q_1 \\ q_2 \end{pmatrix} = \begin{pmatrix} 1 \\ 0 \end{pmatrix}, \tag{14}$$

and

$$p = \begin{pmatrix} p_1 \\ p_2 \end{pmatrix} = \begin{pmatrix} 1 \\ \frac{2b}{3+2(d+\epsilon)} \end{pmatrix}. \tag{15}$$

The components of the multilinear form $B(q,q)$ are given by:

$$[B(q,q)]_1 = \sum_{j,k=1}^{2} \frac{\partial^2 \left(ax(1-x) - \frac{bxy}{1+\epsilon x}\right)}{\partial x_j \partial x_k} q_j q_k = -2a = -6, \tag{16}$$

$$[B(q,q)]_2 = \sum_{j,k=1}^{2} \frac{\partial^2 \left(\frac{dxy}{1+\epsilon x}\right)}{\partial x_j \partial x_k} q_j q_k = -\frac{2dy\epsilon}{(1+\epsilon x)^3} = 0, \tag{17}$$

where the state variable vector is for ease of notation generically denoted by $(x_1, x_2)^T$ instead of $(x, y)^T$.

Let $\zeta = (I-A)^{-1}B(q,q)$, then we have $\zeta = \begin{pmatrix} -3 \\ 0 \end{pmatrix}$ and find

$$[B(q,\zeta)]_1 = -2a(-3) = 18, \quad [B(q,\zeta)]_2 = \frac{6dy\epsilon}{(1+\epsilon x)^3} = 0. \tag{18}$$

The third order multilinear form $C(q,q,q)$ is given by

$$[C(q,q,q)]_1 = \sum_{j,k,l=1}^{2} \frac{\partial^3 \left(ax(1-x) - \frac{bxy}{1+\epsilon x}\right)}{\partial x_j \partial x_k \partial x_l} q_j q_k q_l = \frac{-6by\epsilon^2}{(1+\epsilon x)^4} = 0, \tag{19}$$

$$[C(q,q,q)]_2 = \sum_{j,k,l=1}^{2} \frac{\partial^3 \left(\frac{dxy}{1+\epsilon x}\right)}{\partial x_j \partial x_k \partial x_l} q_j q_k q_l = \frac{6dy\epsilon^2}{(1+\epsilon x)^4} = 0. \tag{20}$$

The critical normal form coefficient b is given by

$$b = \frac{1}{6} p^T \begin{pmatrix} 54 \\ 0 \end{pmatrix} = 9, \tag{21}$$

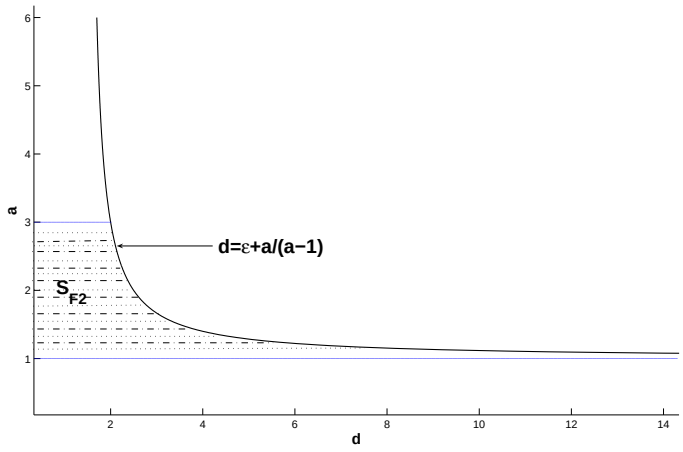

Fig. 1. S_{F2} is the stability region of F_2 for $\epsilon = 0.5$.

which is clearly positive. This completes the proof of supercriticality of the flip point at F_2. □

The stability region S_{F2} of F_2, as obtained in Proposition 2, is shown in Figure 1 for $\epsilon = 0.5$. We note that the supercriticality of the flip bifurcation in Proposition 2 was also obtained in [15] though our proof is different.

2.3 Stability of F_3

To study the stability of F_3 we use the Jury's criteria, see [24], §A2.1. Let $F(\lambda) = \lambda^2 - tr(J(F_3))\lambda + det(J(F_3))$ be the characteristic equation of $J(F_3)$. Hence we have $F(\lambda) = (\lambda - \lambda_1)(\lambda - \lambda_2)$ where λ_1, λ_2 are the eigenvalues of $J(F_3)$.

According to the Jury's criteria F_3 is asymptotically stable if the following conditions hold:

$$\begin{array}{c} F(-1) = 1 + tr(J(F_3)) + det(J(F_3)) > 0, \\ F(1) = 1 - tr(J(F_3)) + det(J(F_3)) > 0, \\ 1 - det(J(F_3)) > 0. \end{array} \tag{22}$$

At F_3 we have:

$$J(F_3) = \begin{pmatrix} a\left(1 - \frac{2}{d-\epsilon}\right) - \frac{d-\epsilon}{d}\left(a\left(1 - \frac{1}{d-\epsilon}\right) - 1\right) & \frac{-b}{d} \\ \frac{d-\epsilon}{b}\left(a\left(1 - \frac{1}{d-\epsilon}\right) - 1\right) & 1 \end{pmatrix}. \tag{23}$$

We note that:

$$tr(J(F_3)) = 1 + a\left(1 - \frac{2}{d-\epsilon}\right) - \frac{d-\epsilon}{d}\left(a\left(1 - \frac{1}{d-\epsilon}\right) - 1\right),$$

and

$$det(J(F_3)) = a\left(1 - \frac{2}{d-\epsilon}\right),$$

are independent of b.

Proposition 3. *F_3 is asympotically stable iff one of the following mutually exclusive conditions holds:*

(i) $\epsilon + \frac{3}{2} < d < \frac{1}{8}\left(4\epsilon + 9 + \sqrt{16\epsilon^2 + 56\epsilon + 81}\right)$ *and*
$\frac{d-\epsilon}{d-\epsilon-1} < a < \frac{(d-\epsilon)(\epsilon-3d)}{2d(d-\epsilon-2)+(d-\epsilon)(-d+\epsilon+1)}$,

(ii) $d = \frac{1}{8}\left(4\epsilon + 9 + \sqrt{16\epsilon^2 + 56\epsilon + 81}\right)$ *and*
$\frac{d-\epsilon}{d-\epsilon-1} < a < \frac{d-\epsilon}{d-\epsilon-2} = \frac{(d-\epsilon)(\epsilon-3d)}{2d(d-\epsilon-2)+(d-\epsilon)(-d+\epsilon+1)}$,

(iii) $d > \frac{1}{8}\left(4\epsilon + 9 + \sqrt{16\epsilon^2 + 56\epsilon + 81}\right)$ *and* $\frac{d-\epsilon}{d-\epsilon-1} < a < \frac{d-\epsilon}{d-\epsilon-2}$.

Proof. The criterion $F(1) > 0$ is easily seen to be equivalent to the condition

$$a > \frac{d-\epsilon}{d-\epsilon-1}, \tag{24}$$

or equivalently,

$$d > \epsilon + \frac{a}{a-1}, \tag{25}$$

i.e. a slightly stronger version of the second condition in (4).

Next, the criterion $\det(J(F3)) < 1$ is easily seen to be equivalent to

$$a < \frac{d-\epsilon}{d-\epsilon-2} \text{ for all } d > \epsilon + 2. \tag{26}$$

The criterion $F(-1) > 0$ translates as

$$a < \frac{(d-\epsilon)(3d-\epsilon)}{(d-\epsilon)(d-\epsilon-1) - 2d(d-\epsilon-2))} \tag{27}$$

for all d, ϵ that satisfy

$$(d-\epsilon)(d-\epsilon-1) - 2d(d-\epsilon-2) > 0. \tag{28}$$

The latter equation is easily seen to be equivalent to

$$d < \frac{3 + \sqrt{9 + 4\epsilon^2 + 4\epsilon}}{2}. \tag{29}$$

It is also easy to see that for a given $\epsilon > 0$ the only values of a, d for which the inequalities in (24) and (27) are both equalities is found for $d = \epsilon + \frac{3}{2}$, $a = 3$.

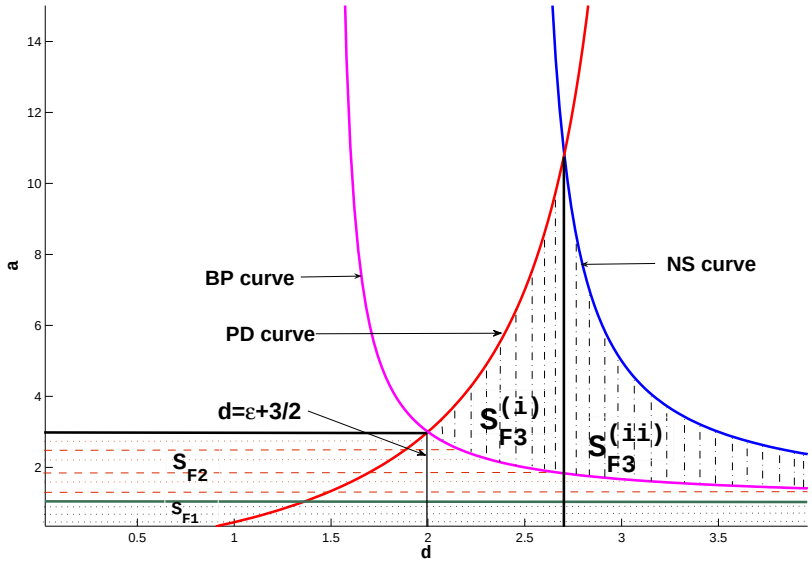

Fig. 2. Stability regions in $(d, a)-$ space for $\epsilon = 0.5$. S_{F1}, S_{F2} are the stability regions of F_1, F_2 respectively. The stability region S_{F3} of F_3 is the union of $S_{F3}^{(i)}$ and $S_{F3}^{(ii)}$ (which correspond to (i) and (iii) in Proposition 3, respectively), and the open interval that separates them (and corresponds to (ii) in Proposition 3). $a = \frac{(d-\epsilon)(3d-\epsilon)}{(d-\epsilon)(d-\epsilon-1)-2d(d-\epsilon-2))}$ indicates the PD curve, $a = \frac{d-\epsilon}{d-\epsilon-2}$ determines the NS curve, $a = \frac{d-\epsilon}{d-\epsilon-1}$ indicates the BP curve and $a = \frac{\epsilon}{2} + \frac{1}{8}\sqrt{9+16\epsilon^2+56\epsilon+81}$ indicates the line that separates the regions $S_{F3}^{(i)}$ and $S_{F3}^{(ii)}$.

Similarly, for a given $\epsilon > 0$ there is a unique pair a, d for which the inequalities in (26) and (27) are both equalities. For this point we have

$$d = \frac{1}{8}(4\epsilon + 9 + \sqrt{16\epsilon^2 + 56\epsilon + 81}), a = \frac{-4\epsilon + \sqrt{16\epsilon^2 + 56\epsilon + 81} + 9}{-4\epsilon + \sqrt{16\epsilon^2 + 56\epsilon + 81} - 7}. \quad (30)$$

□

The stability regions (i) and (iii) of F_3 obtained in Proposition 3 are depicted as $S_{F3}^{(i)}$ and $S_{F3}^{(ii)}$, respectively, in Figure 2 for $\epsilon = 0.5$. The region (ii) is the open interval on the common boundary of $S_{F3}^{(i)}$ and $S_{F3}^{(ii)}$. We note that these regions are qualitatively similar for all values $\epsilon > 0$ and so we have a complete description of the stability region of F_3 for all parameter combinations.

2.4 Notes

Proposition 4 in [1] is somewhat similar to our Proposition 3 but is incomplete and needs several corrections. We give a few examples.

- Consider fixed values $d = 3.5, \epsilon = 1$. For these we have

$$d > \frac{1}{8}\left(4\epsilon + 9 + \sqrt{16\epsilon^2 + 56\epsilon + 81}\right) \approx 3.17116.$$

  By Proposition 3 F_3 is stable when $1.666667 < a < 5$.
  The stability condition in Proposition 4, part (i) in [1] includes the condition

$$a > \frac{(3d-\epsilon)(d-\epsilon)}{(d-\epsilon)(2d-\epsilon) - 2d(d-\epsilon-2)} \approx 2.065217,$$

  so this condition is not necessary.
- For the parameter values $d = 3.7, \epsilon = 2$,

$$\frac{1}{8}\left(4\epsilon + 9 + \sqrt{16\epsilon^2 + 56\epsilon + 81}\right) \approx 4.1289$$

  and so the first condition in part (i) of Proposition 3 is satisfied. The second condition leads to (approximately)

$$2.42857 < a < 4.53665.$$

  But the condition $a < \frac{d-\epsilon}{d-\epsilon-2} = -5.666667$ in Proposition 4, part (i) of [1] can never be satisfied for $a > 0$. Hence that condition is not a necessary one.
- For $d = 3.5, \epsilon = 1$, it is claimed in part (iii) of Proposition 4 in [1] that F_3 is non-hyperbolic if

$$a = \frac{(3d-\epsilon)(d-\epsilon)}{(d-\epsilon)(2d-\epsilon) - 2d(d-\epsilon-2)} \approx 2.06522.$$

  Part (i) of Proposition 3 in fact proves that this is a stable fixed point.
- For $d = 3.5$, $\epsilon = 1$, it is claimed in part (iv) of Proposition 4, in [1] that F_3 is a saddle if $a < \frac{(3d-\epsilon)(d-\epsilon)}{(d-\epsilon)(2d-\epsilon)-2d(d-\epsilon-2)} \approx 2.06522$. Part (i) of Proposition 3 in fact proves that this is a stable fixed point for values of a slightly below 2.06522.

2.5 Bifurcations of F_3

Proposition 4. *Suppose that the conditions (4) hold. Then F_3 loses stability:*

(i) via a flip point when $a = \dfrac{(d-\epsilon)(3d-\epsilon)}{(d-\epsilon)(d-\epsilon-1) - 2d(d-\epsilon-2)}$ *and* $\epsilon + \dfrac{3}{2} < d < \dfrac{1}{8}\left(4\epsilon + 9 + \sqrt{16\epsilon^2 + 56\epsilon + 81}\right)$,

(ii) via a Neimark-Sacker bifurcation when $a = \dfrac{d-\epsilon}{d-\epsilon-2}$ *and* $d > \dfrac{1}{8}\left(4\epsilon + 9 + \sqrt{16\epsilon^2 + 56\epsilon + 81}\right)$,

(iii) via branching when $a = \dfrac{d-\epsilon}{d-\epsilon-1}$ *and* $d > \epsilon + \dfrac{3}{2}$, *where it bifurcates to* F_2,

(iv) via a fold-flip (LPPD) point when $d = \epsilon + \dfrac{3}{2}$ *and* $a = 3$,

(v) via a resonance 1:2 point when $d = \dfrac{1}{8}\left(4\epsilon + 9 + \sqrt{16\epsilon^2 + 56\epsilon + 81}\right)$ *and* $a = \dfrac{-4\epsilon + \sqrt{16\epsilon^2 + 56\epsilon + 81} + 9}{-4\epsilon + \sqrt{16\epsilon^2 + 56\epsilon + 81} - 7}$.

Proof. By Proposition 3 (see also Figure 2) the stability boundary of F_3 consists of parts of three curves, namely

1. Curve 1: $a = \frac{(d-\epsilon)(3d-\epsilon)}{(d-\epsilon)((d-\epsilon-1))-2d(d-\epsilon-2)}$,
2. Curve 2: $a = \frac{d-\epsilon}{d-\epsilon-2}$,
3. Curve 3: $a = \frac{d-\epsilon}{d-\epsilon-2}$.

The points of Curve 1 which are on the stability boundary of F_3 satisfy $F(-1) = 0$, i.e. they have an eigenvalue -1. The points of Curve 2 which are on the stability boundary satisfy $\det(J(F_3)) = 1$, i.e. they have two eigenvalues with product 1. The points of Curve 3 which are on the stability boundary satisfy $F(1) = 0$, i.e. they have an eigenvalue $+1$.

Combining this with Proposition 2 we find that the interior points of the boundary parts of Curves 1,2, and 3 form the sets described in parts (i), (ii) and (iii) of the Proposition, respectively.

Next, Curves 1 and 3 have an intersection point which has eigenvalues $+1$ and -1. This is the $LPPD$ point in part (iv) of the Proposition (but note that it is degenerate, in fact a $BPPD$ point).

Finally, Curves 1 and 2 also have an intersection point. In this point both eigenvalues are -1. This is the $1:2$(R2) in part (v) of the the Proposition. □

We remark that our numerical evidence indicates that the flip and Neimark-Sacker bifurcations in *Proposition 4* are sub- and supercritical, respectively in all cases considered in this paper. This is based on the numerical computation of the normal form coefficients of these bifurcations (see [19], Ch. 8 and [8]). However, a detailed study in [15] (Theorem 4.1 and Theorem 5.1) suggests that other cases might be possible for certain combinations of parameter values. Resonances are also possible, cf. §3.2 and the discussion at the end of §5 in [15].

We further note that in the case $\epsilon = 0$ our model (2) reduces to model (7) in [25] under a rescaling of the $x-$ variable and introduction of the parameters c, r with $a = r + 1$, $b = c$, $d = (r + 1)c/r$. By straightforward calculations one finds that the new equations for the PD, BP and NS curve then must be replaced by $c = 3r/(r + 4)$, $c = 1$, and $c = 2$, respectively. Hence we exactly reproduce the results summarized in Figure 1 of [25]. We note, however, that in [25] the subcriticality of the PD bifurcations is proved (for $\epsilon = 0$).

Model (30) in [25] uses the parameters c, r, γ. It is equivalent to (2) under a rescaling of the $x-$ variable and by setting $a = r + 1$, $b = c/\gamma$, $\epsilon = (r + 1)/(r\gamma)$, $d = c(r + 1)/(r\gamma)$. In [25] the stability region of F_3 is depicted in $(r, c)-$ space in the case $\gamma = 1$ and it is mentioned that subcritical flip points were found in this case.

The case $\epsilon = 0$ also reduces to model (1) in [23] (in terms of the parameters α, β where $a = \alpha$, $b = 1$, $d = 1/\beta$). We note, however, that in [23] the supercriticality of the NS bifurcations is proved (for $\epsilon = 0$).

In the sequel we will concentrate on the numerical study of cycles and their stability since this leads to finding parameter regions where stable periodic behaviour with different periods is found.

3 Numerical bifurcation analysis of F_2 and F_3

In this section we perform a numerical bifurcation analysis by using the MATLAB package MatContM, see [8] and [9]. The bifurcation analysis is based on continuation methods, tracing out the solution manifolds of fixed points while some of the parameters of the map vary, see [2].Testruns for these computations willl be made available via [9].

3.1 Numerical bifurcation of F_2

We continue $F_2 = (0.54545454, 0)$ starting with $a = 2.2, b = 3, \epsilon = 0.2, d = 0.5$ with a free. We see that F_2 is stable when $1 < a < 3$. It loses stability via a supercritical period doubling point when $a = 3$, and via a branch point when a crosses 1. These results are consistent with Proposition 2 since $d < \epsilon + \frac{3}{2} \leq d + \frac{a}{a-1}$ for all $a \in]1, 3[$. The output of *Run 1* is given by:

```
label = BP  , x = ( -0.000000 -0.000000 1.000000 )
label = PD  , x = ( 0.666667 0.000000 3.000000 )
normal form coefficient of PD = 9.000000e+000
```

The first two entries of $\mathbf{x}$ are the coordinate values of the fixed point F_2, and the last entry of $\mathbf{x}$ is the value of the free parameter a at the corresponding bifurcation point. We note that the normal form coefficient of the PD point is 9, confirming (21). The curve computed in *Run 1* is presented in Figure 3. Beyond the PD point the dynamics of (2) is a stable 2-cycle. MatContM allows to switch to the continuation of this 2-cycle. It loses stability at a supercritical PD point for $a = 3.449490$. A stable 4-cycle is born when $a > 3.449490$. An instance is given by $C_4 = \left\{X_1^4, X_2^4, X_3^4, X_4^4\right\}$ where $X_1^4 = (0.87867696, 0), X_2^4 = (0.37483245, 0)$, $X_3^4 = (0.82394508, 0), X_4^4 = (0.51004805, 0)$. The correponding parameter values are $a = 3.516128, b = 3, \epsilon = 0.2, d = 0.5$. We note that the $y-$coordinate equals zero in all four points of the cycle. The 4-cycle loses stability via a supercritical PD point for $a = 3.544090$. Thus, when $a > 3.544090$ a stable 8-cycle emerges. This 8-cycle loses stability at another supercritical PD point for $a = 3.564407$. In fact a cascade of period doublings appears if we further

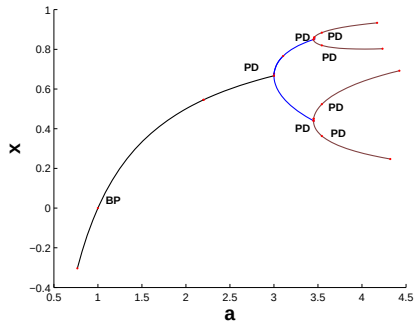

Fig. 3. Continuation of F_2 in (x, a)-space.

increase a. We note that for F_2 the map (2) is a logistic map, which is well know to have chaotic behavior through a cascade of period doubling points, see [18].

Continuation of F_2 starting from the same parameter values as in *Run 1*, with d as free parameter, leads to the discovery of a branch point for $d = 2.033333$. This is consistent with Proposition 2 part (ii) which states that F_2 bifurcates to F_3 when $d = \epsilon + \frac{a}{a-1} = 0.2 + \frac{2.2}{1.2} = 2.033333$.

3.2 Numerical bifurcation of F_3

We now consider $F_3 = (0.4, 0.681333)$ which is in the stable region for the parameter values $a = 4.1, b = 3, \epsilon = 1, d = 3.5$ (stability follows from Proposition 3 part (i)). We do a numerical continuation of F_3 with control parameter ϵ, and call this *Run 2*:

```
label = NS  , x = ( 0.378049 0.683638 0.854839 )
normal form coefficient of NS = -9.079782e+000
label = PD  , x = ( 0.603958 0.439521 1.844256 )
normal form coefficient of PD = -7.976577e+000
label = BP  , x = ( 0.756098 0.000000 2.177419)
```

F_3 is stable when $0.854839 < \epsilon < 1.844256$. It loses stability via a supercritical Neimark-Sacker (NS) point when $\epsilon = 0.854839$, which is consistent with Proposition 4 part (ii) ($\frac{d-\epsilon}{d-\epsilon-2} = 4.1 = a$). It loses stability through a subcritical PD point when $\epsilon = 1.844256$, which is consistent with Proposition 4 part (i) since $\frac{(d-\epsilon)(3d-\epsilon)}{(d-\epsilon)(d-\epsilon-1)-2d(d-\epsilon-2)} = 4.1 = a$.

The dynamics of the system prior to the PD point consists of an unstable 2-cycle that coexists with a stable fixed point. For $\epsilon < 0.854839$, a stable closed invariant curve is created around the unstable fixed point F_3. Such a curve is shown in Figure 4. Now we compute the period doubling curve, with a and ϵ free, by starting from the PD point detected in *Run 2*. We call this *Run 3*.

```
label = LPPD, x = ( 0.666667 0.000000 3.000000 2.000000 )
```

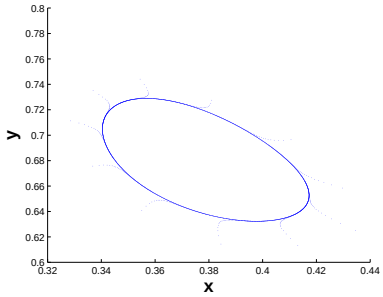

Fig. 4. The stable closed invariant curve for $a = 4.1, b = 3, \epsilon = 0.84, d = 3.5$.

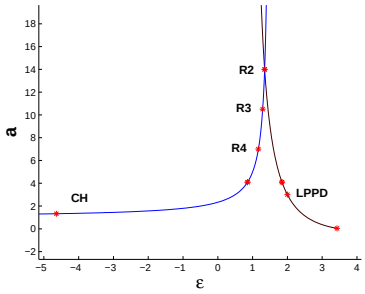

Fig. 5. Flip and Neimark-Sacker bifurcation curves starting from points in *Run 2* .

```
Normal form coefficient for LPPD :[a/e , be]=
 -1.200000e-001, -3.467480e-006,
label = R2  , x = ( 0.464286 3.520833 14.000000 1.346154 )
Normal form coefficient for R2 :[c , d]= 3.479148e+001, -1.346125e+002
```

Two codim-2 bifurcation points are detected on the flip curve, namely a fold-flip $LPPD$ and a resonance 2 bifurcation $R2$, see Figure 5 (right curve). We note that the $LPPD$ point is degenerate in the sense that it is really a $BPPD$ point. The parameter values indeed satisfy the equation $a = (d - \epsilon)/(d - \epsilon - 1)$ of the branch point curve, cf. Proposition 4. In general, a $BPPD$ point is ungeneric on a PD curve and therefore is not detected by the software. It follows that the normal form coefficients given for the pretended $LPPD$ point are meaningless.

Now we compute the NS curve, with a and ϵ free parameters, by starting from the NS point of *Run 2*. We call this *Run 4*.

```
label = R4  , x = ( 0.428571 1.500000 7.000000 1.166667 -0.000000 )
Normal form coefficient of R4 : A = -1.260354e+000 + 7.511202e-001 i
label = R3  , x = ( 0.452381 2.506944 10.500000 1.289474 -0.500000 )
Normal form coefficient of R3 : Re(c_1) = -5.439941e-001
label = R2  , x = ( 0.464286 3.520833 13.999998 1.346154 -1.000000 )
Normal form coefficient of R2 : [c , d] = 3.479148e+001, -1.346125e+002
label = CH  , x = ( 0.122849 0.023342 1.325730 -4.640055 0.810610 )
Normal form coefficient of CH = 9.285903e+001
```

The computed curve of NS points is also shown in Figure 5 (left curve). We note that the PD and NS curves intersect in an $R2$ point. The codim-2 bifurcations that are computed along the Neimark-Sacker curve are a resonance 1:2 ($R2$), resonance 1:3 ($R3$), resonance 1:4 ($R4$) and a Chenciner bifurcation (CH). In addition to the coordinates of the bifurcation point, parameter values and the real part of the Neimark-Sacker multiplier at the bifurcation point are output.

A closer look at the codimension 2 bifurcations found in this subsection reveals that the Chenciner bifurcation is far away in an ecologically impossible

parameter region. For the $LPPD$ bifurcation it follows from the output $be < 0$ that no new local bifurcation curves are rooted in this point, cf. [8]. Similarly, for the $R2$ bifurcation the output $c > 0$ has the same implication. We therefore concentrate on the remaining cases $R4$ and $R3$.

3.3 Orbits of period 4, 8 and 16

In this subsection we will describe parameter regions where predator and prey can coexist in a stable way and reproduce their densities every fourth, eighth or sixteenth years. The regions with 4-cycle and 8-cycle stability overlap, so that bistability occurs. The normal form coefficient A of the $R4$ point in *Run 4* satisfies $|A| > 1$, hence two cycles of period 4 of the map are born. A stable 4-cycle for $a = 6.401280, b = 3, \epsilon = 1.093117$ and $d = 3.5$ is given by: $C_4 = \{X_1, X_2, X_3, X_4\}$ where $X_1 = (0.347307, 1.272391)$.In order to compute the stability region of this 4-cycle, we compute two fold curves of the fourth iterate rooted at the $R4$ point. These curves exist since $|A| > 1$, see [19] and switching from an $R4$ point to the fold curves of the fourth iterate is supported by MatContM. The stable fixed points of the fourth iterate exist in the wedge between the two fold curves. The output of this continuation, *Run 5*, is given below and the fold curves (denoted by LP^4) are shown in Figure 7.

```
label = LPPD, x = ( 0.341617 1.808057 7.596591 1.084004 )
Normal form coefficient for LPPD :[a/e , be]= 5.904006e-001, -4.511886e+001,
label = LPPD, x = ( 0.085157 0.508424 3.947668 -0.035122 )
Normal form coefficient for LPPD :[a/e , be]= -1.863197e-001, -2.336863e+003,
```

We can further compute the stability boundaries of the 4-cycle. This region is bounded by the two just computed limit point curves and a period doubling curve of the fourth iterate rooted at the detected $LPPD$ points on the branches of LP^4 curves.

Continuation of the flip curve of the fourth iterate emanated at the $LPPD$ of *Run 5* is given below. We call this *Run 6*.

```
label = GPD , x = ( 0.341591 1.802206 7.570354 1.087021 )
Normal form coefficient of GPD = 8.180449e+005
label = R2  , x = ( 0.317814 1.734061 7.225039 1.068919 )
Normal form coefficient for R2 :[c , d]= -2.430015e+002, -1.078458e+003
label = GPD , x = ( 0.311884 1.760666 7.295843 1.056324 )
Normal form coefficient of GPD = -3.64862e+004
```

This curve is depicted in Figure 7 and indicated by PD^4 curve. We further compute a curve of fixed points of the fourth iterate starting from the 4-cycle C_4 with control parameter a. We call this *Run 7*. The curve is presented in Figure 6.

The 4-cycle is stable in the wedge between the two LP^4 curves, and loses stability when crossing the PD^4 curve. When C_4 loses stability at the super-critical PD point corresponding to $a = 7.284657$, a stable 8-cycle is born which coexists with an unstable 4-cycle until the second PD point ($a = 7.483037$) is reached. A stable 8-cycle is given by $C_8 = \left\{X_1^8, X_2^8, X_3^8, X_4^8, X_5^8, X_6^8, X_7^8, X_8^8\right\}$

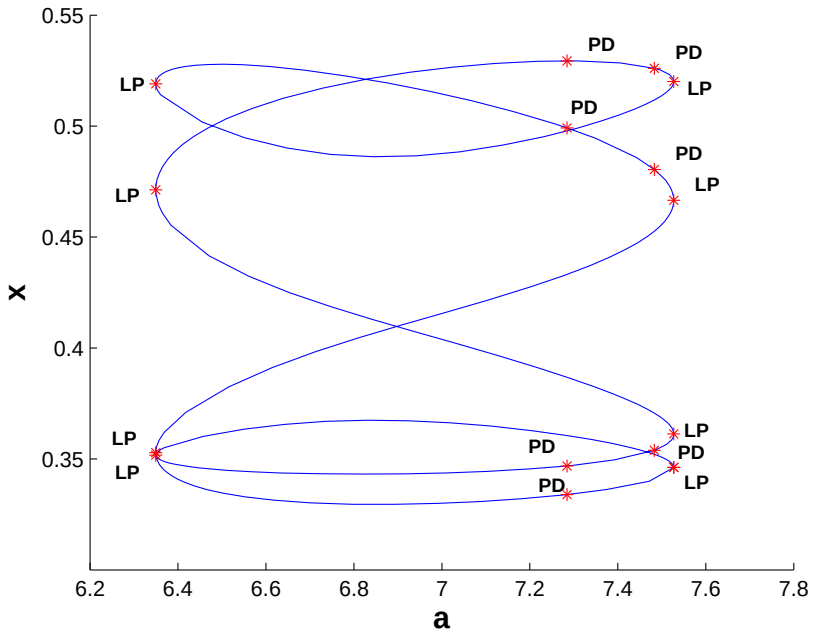

Fig. 6. Curve of fixed points of the fourth iterate starting from the 4-cycle C_4.

where $X_1^8 = (0.510422, 1.384081)$ for $a = 7.411918, b = 3, \epsilon = 1.093117$ and $d = 3.5$. We can compute the stability boundaries of C_8, by computing two fold curves of the eighth iterate by switching at the GPD points in *Run 6*. Again, this is supported by MatcontM. These fold curves emanate tangentially to the fold curve of the fourth iterate in *Run 6*. These curves are presented in Figure 7 and indicated by LP^8 curves. The region where C_8 is stable is bounded by the two fold curves of the eighth iterate and the lower part of the flip curve of the fourth iterate (shaded region indicated by Ω_S^8).

Further we continue the 4-cycle (C_4) with control parameter ϵ. The output of this continuation, *Run 8*, is:

```
label = NS   , x = ( 0.328281 1.215657 1.057947 )
 normal form coefficient of NS = -4.089749e+002
label = LP   , x = ( 0.355258 1.300254 1.100154 )
normal form coefficient of LP =-7.154929e+000
```

The 4-cycle remains stable when $1.057947 < \epsilon < 1.100154$. Now we compute a NS-curve starting from the computed NS point in *Run 8*, given below. This curve is depicted in Figure 7 and indicated by NS^4 curve. We call this *Run 9*.

```
label = R3   , x = ( 0.331234 1.257772 6.541014 1.066957 -0.500000 )
Normal form coefficient of R3 : Re(c_1) = -4.885966e+000
```

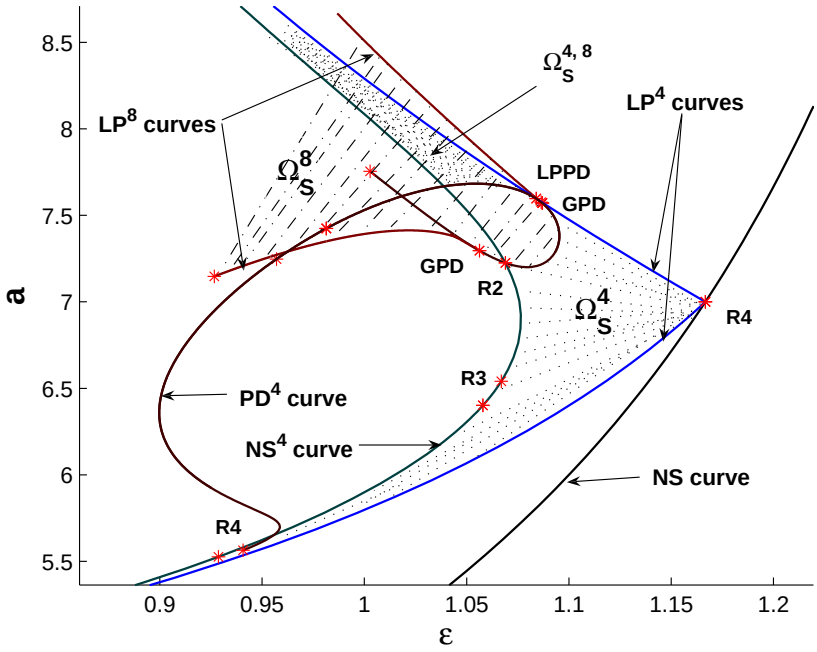

Fig. 7. Bifurcation curves of NS, two branches of LP^4 emanating at the R_4, PD^4 rooted at the $LPPD$ points, two branches of LP^8 which are born tangentially at the GPD points. These curves form stability boundaries of 4-cycle ($\Omega_S^4 \cup \Omega_S^{4,8}$) and 8-cycle ($\Omega_S^8$) and bistability of 4-cycle and 8-cycle ($\Omega_S^{4,8}$).

```
label = R2   , x = ( 0.332363 1.439768 7.225039 1.068919 -1.000000 )
Normal form coefficient of R2 : [c , d] = -1.046630e+002, -4.653504e+002
label = R4   , x = ( 0.294522 0.915737 5.526230 0.928728 0.000000 )
Normal form coefficient of R4 : A = -4.055960e+000 + -8.600805e-001 i
```

We note that we have bistability of the 4-cycle (C_4) and 8-cycle (C_8) in the region indicated by $\Omega_S^{4,8}$ in Figure 7. We note that the NS curve of the fourth iterate in *Run 9* and the PD curve of the fourth iterate of *Run 6* intersect in an $R2$ point. Now we consider the $R4$ point computed in *Run 9*. Since $|A| > 1$ (A is the corresponding normal form coefficient of the $R4$ point), two cycles of period 16 of the map are born. A stable 16-cycle is given in Figure 8. In order to compute the stability region of this 16-cycle, we compute two fold curves of the sixteenth iterate rooted at the $R4$ point. These curves exist since $|A| > 1$. The stable fixed points of the sixteenth iterate exist in the wedge between the two fold curves. The output of this continuation, *Run 10* is given below. The fold curves are shown in Figure 9.

```
label = LPPD, x = ( 0.294382 0.903595 5.468882 0.911109 )
```

```
Normal form coefficient for LPPD :[a/e , be]= 4.600977e+000, -1.127121e+002,
label = R1   , x = ( 0.221519 0.406043 4.347547 0.363383 )
normal form coefficient of R1 = -1
label = LPPD, x = ( 0.222150 0.409925 4.354848 0.368810 )
Normal form coefficient for LPPD :[a/e , be]= -5.087744e-001, -1.179672e+009,
label = R1   , x = ( 0.181745 0.167415 3.975582 -0.000054 )
normal form coefficient of R1 = -1
label = LPPD, x = ( 0.302337 0.997939 5.668515 0.954589 )
Normal form coefficient for LPPD :[a/e , be]= 3.260385e+001, -1.518085e+001,
label = LPPD, x = ( 0.324821 1.218070 6.191127 1.018418 )
Normal form coefficient for LPPD :[a/e , be]= -8.188768e-001, -3.916020e+005,
label = CP   , x = ( 0.338557 1.721717 7.495970 1.027620 )
Normal form coefficient of CP s= -7.702949e+003
```

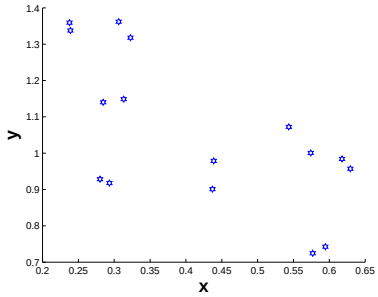

Fig. 8. A stable 16-cycle near the $R4$ point of *Run 9* for $a = 5.549119387672505, b = 3, \epsilon = 0.930418649464793, d = 3.5$.

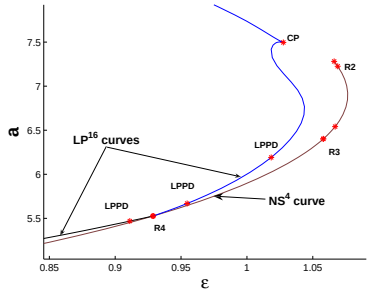

Fig. 9. Two fold curves (LP^{16}) emanate from an $R4$ point.

We note in particular the existence of a cusp point of 16-cycle.

3.4 Orbits of period 3

Next we consider the resonance 1:3 ($R3$) point in *Run 4*. Since its normal form coefficient is negative, the bifurcation picture near the $R3$ point is qualitatively the same as presented in [19], Fig. 9.12. In particular, there is a region near the $R3$ point where a stable invariant closed curve coexists with an unstable fixed point. For parameter values close to the $R3$ point, the map has a saddle cycle of period three.

Furthermore, a curve of Neutral Saddles of fixed points of the third iterate emanates [19], Ch 9. We compute this curve by branch switching at the $R3$ point. This curve is presented in Figure 10. We note that, however interesting, it is not a bifurcation curve.

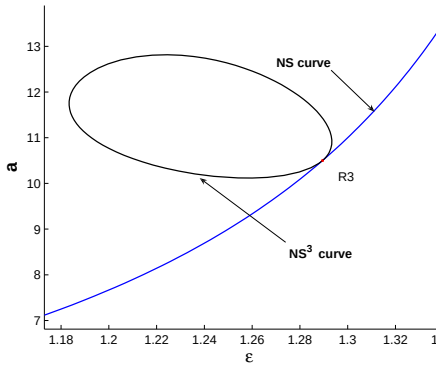

Fig. 10. Curve of Neutral Saddles of the third iterate.

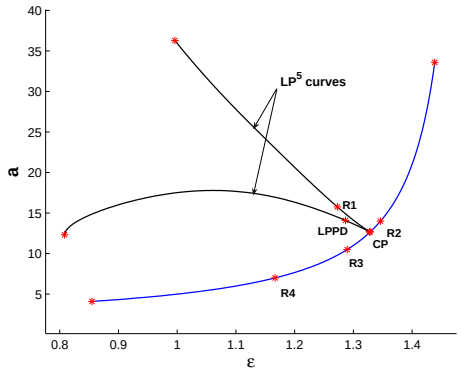

Fig. 11. An Arnol'd tongue rooted in a weak 2 : 5 resonant Neimark-Sacker point.

3.5 Computation of Arnol'd tongues

It is well known that near a Neimark-Sacker curve there exists a dense array of resonance tongues, generalizing the isolated tongue of period 4 in Figure 7. So far, no numerical methods have been implemented to specifically compute the boundaries of the resonance tongues that are rooted in weakly resonant Neimark-Sacker points (unlike the strong resonant 1 : 4 case). However, since they are limit point curves of fixed points of cycles with known periods, they can be computed relatively easily if the cycles inside the tongue are globally stable (which depends on the criticality of the Neimark-Sacker curve and the noncritical multipliers as well). It is sufficient to find a fixed point of cycles inside the tongue by orbit convergence and to continue it in one free parameter to find a point on the boundary of the Arnol'd tongue as a limit point of cycles. From this, the boundary curves can be computed by a continuation in two free parameters. In Figure 11 we present an Arnol'd tongue rooted in a weak 2 : 5 resonant Neimark- Sacker point. Its computation started from a stable 5-cycle with $x = 0.460832, y = 3.136574, a = 12.7, b = 3, \epsilon = 1.327634$, and $d = 3.5$. We note that the boundary curves contain further bifurcation points.

From the ecological point of view, this means that we have described a parameter region where predator and prey can coexist in a stable way and reproduce their densities every fifth year.

4 Concluding remarks

We investigated the dynamical behaviour of a discrete-time predator-prey model with Holling type II functional response. In Section 2, we focused on the stability and possible bifurcations of three types of fixed points of the model denoted

F_1, F_2 and F_3 respectively. We established the stability condition and branching behaviour of F_1 in Proposition 1. Conditions under which F_2 may bifurcate to a flip or a branch point, are derived in Proposition 2. We proved supercriticality of the flip bifurcations of F_2 by computing the corresponding normal form coefficient. Proposition 3 provides the necessary and sufficient conditions under which F_3 is stable. All possible bifurcations of F_3 are given in Proposition 4. In Section 3, we computed curves of fixed points and codim 1 bifurcations of cycles. In particular, we computed curves of flip and Neimark-Sacker bifurcations of the fourth iterate and fold curves of the fourth, eighths and sixteenth iterates. We computed two curves of folds of the eighth iterate that are born tangentially at GPD points on the flip curve of the fourth iterate. These curves bound the stability region of an 8-cycle that is born when a fixed point of the fourth iterate crosses a supercritical flip point. We note the bistability of the 4- and 8-cycles in Figure 7 . Furthermore, curves of fold points of the sixteenth iterate are computed which bound the stability region of a 16-cycle that appears near a resonance 4 point of the fourth iterate. Finally, we described a parameter region inside an Arnol'd tongue where stable 5-cycles of the map occur.

5 Acknowledgment

We thank two referees for several detailed remarks that led to a substantial improvement in the content as well as the presentation of the paper. The first author thanks Shahrekord University (Iran) for the financial support through a research grant.

References

1. H. N. Agiza, E. M. Elabbasy, H. EL-Metwally, and A. A. Elsadany, Chaotic dynamics of a discrete prey-predator model with Holling type II, Nonlinear Analysis: Real World Applications 10(2009)116-129.
2. E. L. Allgower, K. Georg, Numerical Continuation Methods: An Introduction (1990), Springer-Verlag.
3. M. Danca, S. Codreanu, B. Bako, Detailed analysis of a nonlinear prey-predator model, J. Biol. Phys. 23 (1997) 11-20.
4. L. Edelstein-Keshet, 2005, Mathematical Models in Biology (Philadelphia, PA: SIAM).
5. E. M. Elabbasy, S. H. Saker, Dynamics of a class of non-autonomous systems of two non-interacting preys with common predator,J. Appl. Math. Comput. 17 (2005) 195-215.
6. H. Gao, H. Wei, W. Sun and X. Zhai, Functions used in biological models and their influence on simulations, Indian Journal of Marine Science 29 (2000), pp. 230-237.
7. K. Gopalsamy, Stability and Oscillations in Delay Differential Equations of Population Dynamics, Kluwer Academic, Dordrecht, Norwell, MA, 1992.
8. W. Govaerts, R. Khoshsiar Ghaziani, Yu. A. Kuznetsov, and H. G. E. Meijer, Numerical Methods for Two-Parameter Local Bifurcation Analysis of Maps, Siam J. Sci. Comp. 29,6 (2007) 2644-2667.

9. W. Govaerts and Yu. A. Kuznetsov, MatCont: a Matlab software project for the numerical continuation and bifurcation study of continuous and discrete parameterized dynamical systems, www.sourceforge.net.
10. K. P. Hadeler and I. Gerstmann (1990), The discrete Rosenzweig model, Math. Biosci. 98, 49-72.
11. C. S. Holling, The functional response of predator to prey density and its role in mimicry and population regulation. Mem. Ent. Soc. Canada, 45 (1965) 1-60.
12. S. B. Hsu, T.W. Hwang, Global stability for a class of predator-prey systems, SIAM J. Appl. Math. 55 (1995) 763-783.
13. S. R. J. Jang, 2006, Allee effects in a discrete-time host-parasitoid model. Journal of Difference Equations and Applications, 12(2), 165-181.
14. M. Kot, 2001, Elements of Mathematical Ecology, Cambridge University Press, Cambridge.
15. S. Li and W. Zhang, 2010, Bifurcations of a discrete prey-predator model with Holling Type II functional response, Discr. Cont. Dyn. Syst. 14, 159-176.
16. X. Liu, D. Xiao, Complex dynamic behaviors of a discrete-time predator-prey system, Chaos, Solitons and Fractals 32 (2007) 80-94.
17. A.J. Lotka, Elements of Mathematical Biology, Dover, New York, 1926.
18. R. L. Kraft, Chaos, Cantor Sets, and Hyperbolicity for the Logistic Maps. Amer. Math. Monthly 106, 400-408, 1999.
19. Yu. A. Kuznetsov, Elements of Applied Bifurcation Theory, 3rd edition (2004), Springer-Verlag, New York.
20. K. G. Magnusson and O.K. Palsson, Predator-prey interactions of cod and capelin in Icelandic waters, ICES Marine Science Symposium 193 (1991), pp. 153-170.
21. J. Maynard Smith (1968), Mathematical ideas in biology, Cambridge University Press.
22. R. E. Mickens, 2003, A nonstandard finite-difference scheme for the Lotka-Volterra system. Applied Numerical Mathematics, 45, 309-314.
23. K. Murakami, 2007, Stability and bifurcation in a discrete-time predator-prey model, J. Diff. Eqns Appl. 10, 911-925.
24. J. D. Murray, 1993, Mathematical Biology, 2nd corrected edition, Berlin, Heidelberg, New York: Springer.
25. M. G. Neubert and M. Kot, 1992, The subcritical collapse of predator populations in discrete-time predator-prey models, Math. Biosci. 110, 45-66.
26. M. Rosenzweig, 1971, Paradox of enrichment: destabilization of exploitation ecosystems in ecological time, Science 171, 385-387.
27. R. J. Sacker, and H. F. Von Bremen, 2003, A new approach to cycling in a 2-locus 2-allele genetic model. Journal of Difference Equations and Applications, 9(5), 441-448.
28. D. Summers, C. Justian, H. Brian, Chaos in periodically forced discrete-time ecosystem models, Chaos, Solitons and Fractals 11 (2000) 2331-2342.
29. Y. Takeuchi, Global Dynamical Properties of Lotka-Volterra Systems, World Scientific, Singapore, 1996.
30. V. Volterra, Opere matematiche: mmemorie e note, vol. V, Acc. Naz. dei Lincei, Roma, Cremon, 1926.